

Supporting Information

Renal-Clearable Ultra-Small Coordination Polymer Nanodots for Chelator-Free ^{64}Cu -Labeling and Imaging-Guided Enhanced Radiotherapy of Cancer

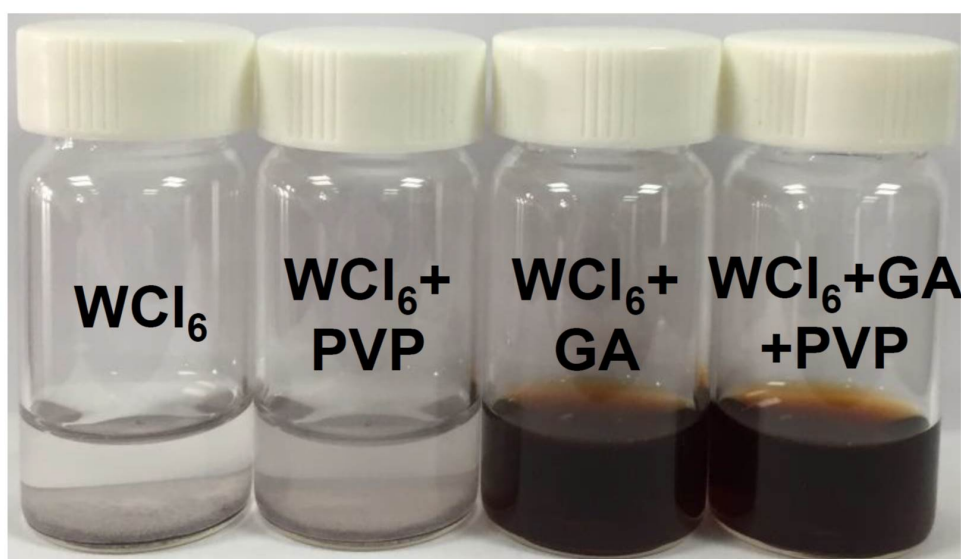
Sida Shen¹, Dawei Jiang^{2,3}, Liang Cheng^{1*}, Yu Chao¹, Kaiqi Nie¹, Ziliang Dong¹, Christopher J. Kuttyreff², Jonathan W. Engle², Peng Huang³, Weibo Cai^{2*}, and Zhuang Liu^{1*}

¹Institute of Functional Nano & Soft Materials (FUNSOM), Collaborative Innovation Center of Suzhou Nano Science and Technology, Soochow University, Suzhou, Jiangsu 215123, China

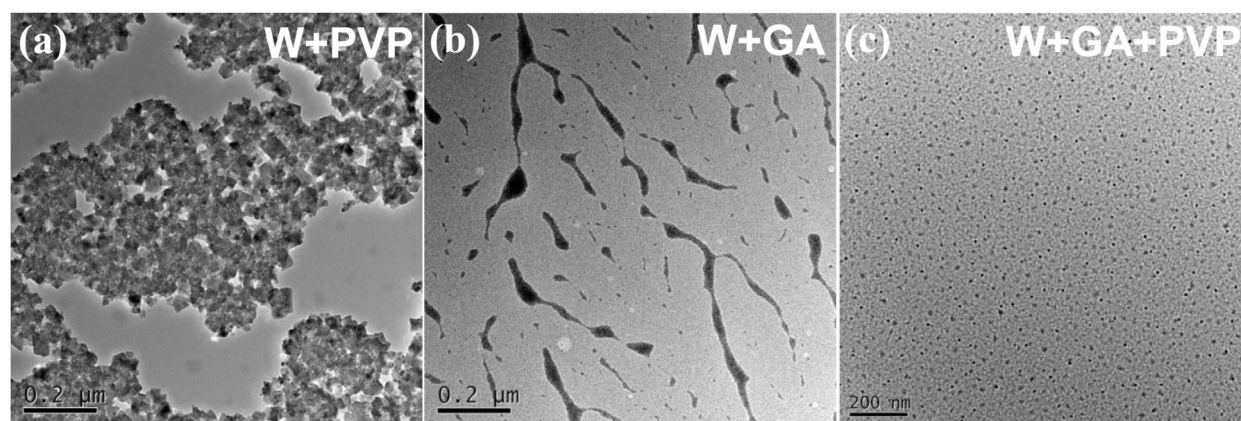
²Departments of Radiology and Medical Physics, University of Wisconsin-Madison, Wisconsin 53705, United States

³Guangdong Key Laboratory for Biomedical Measurements and Ultrasound Imaging, School of Biomedical Engineering, Health Science Center, Shenzhen University, Shenzhen 518060, China

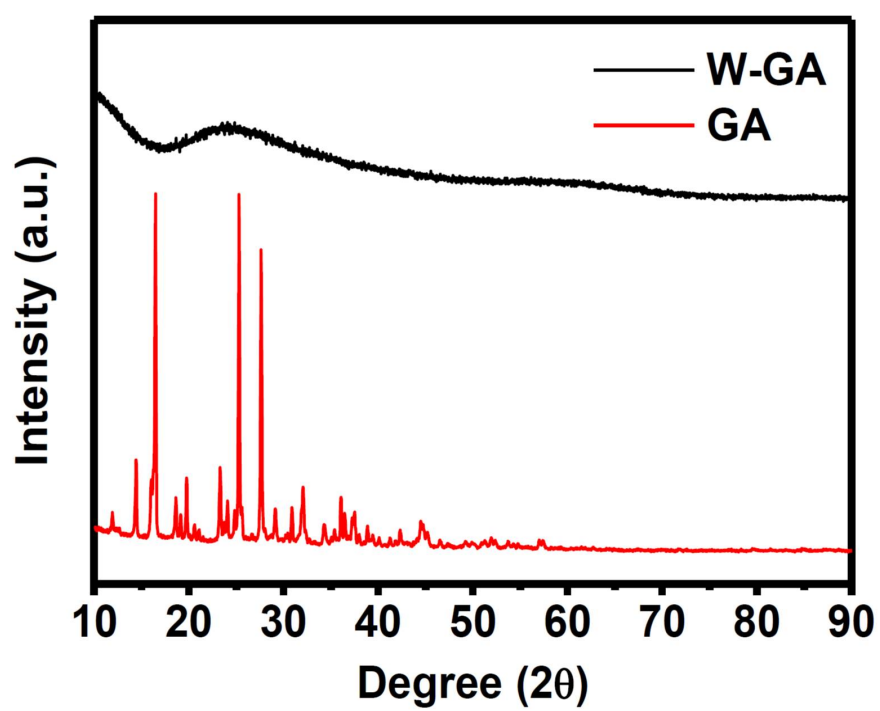
Email: lcheng2@suda.edu.cn; zliu@suda.edu.cn; wcai@uwhealth.org



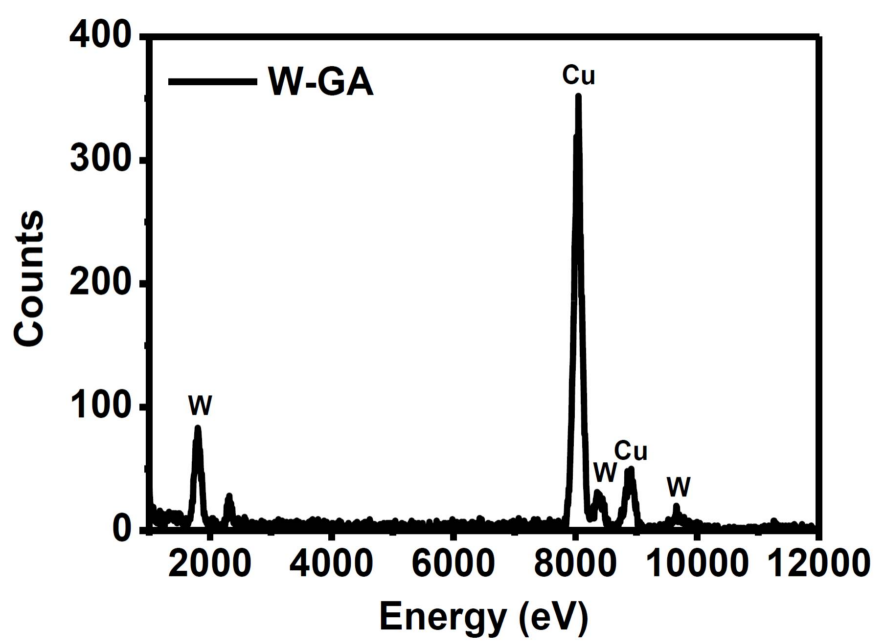
Supporting Figure S1. A Photograph of samples by mixing WCl_6 , WCl_6 +PVP, WCl_6 +GA, and WCl_6 +GA+PVP in water under room temperature.



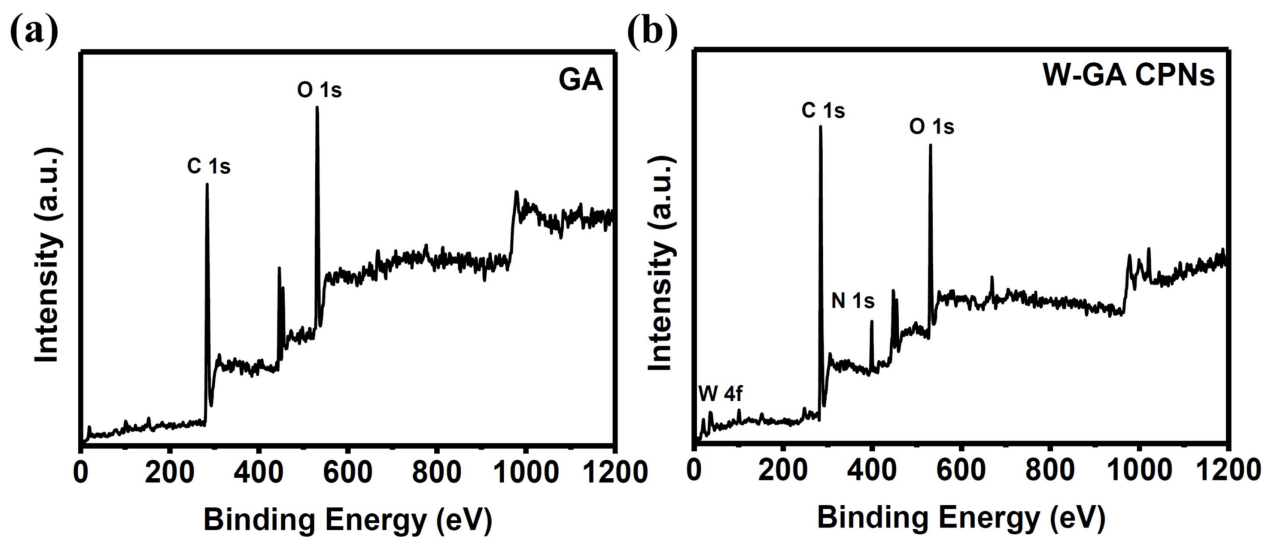
Supporting Figure S2. TEM images of samples by mixing (a) WCl_6 +PVP, (b) WCl_6 +GA, (c) WCl_6 +GA+PVP.



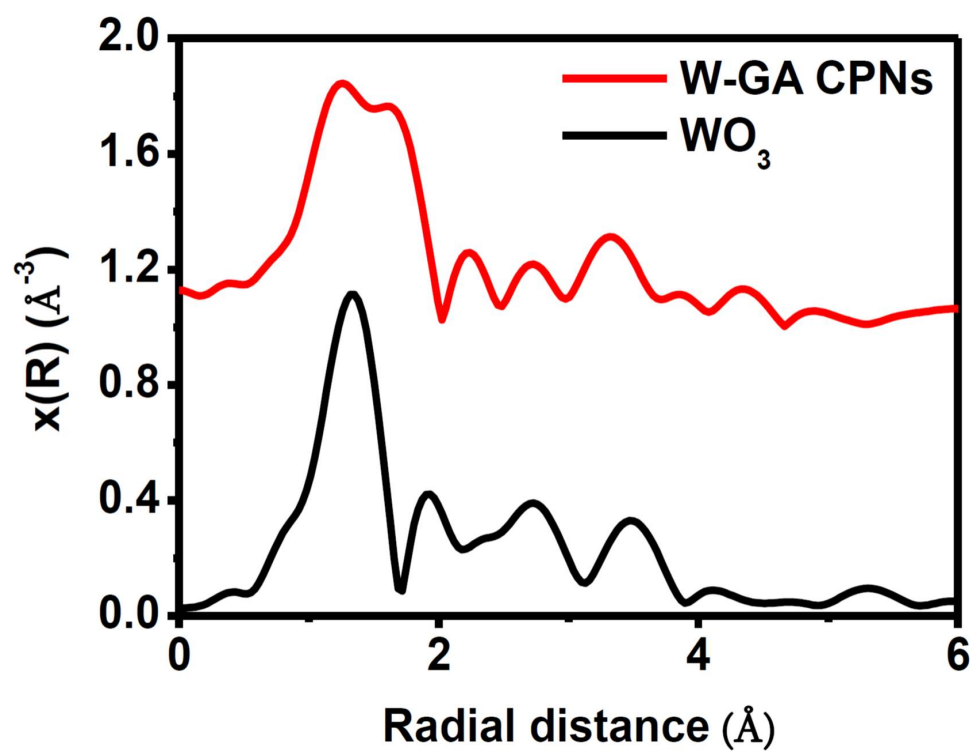
Supporting Figure S3. XRD spectra of GA and as-made W-GA CPNs.



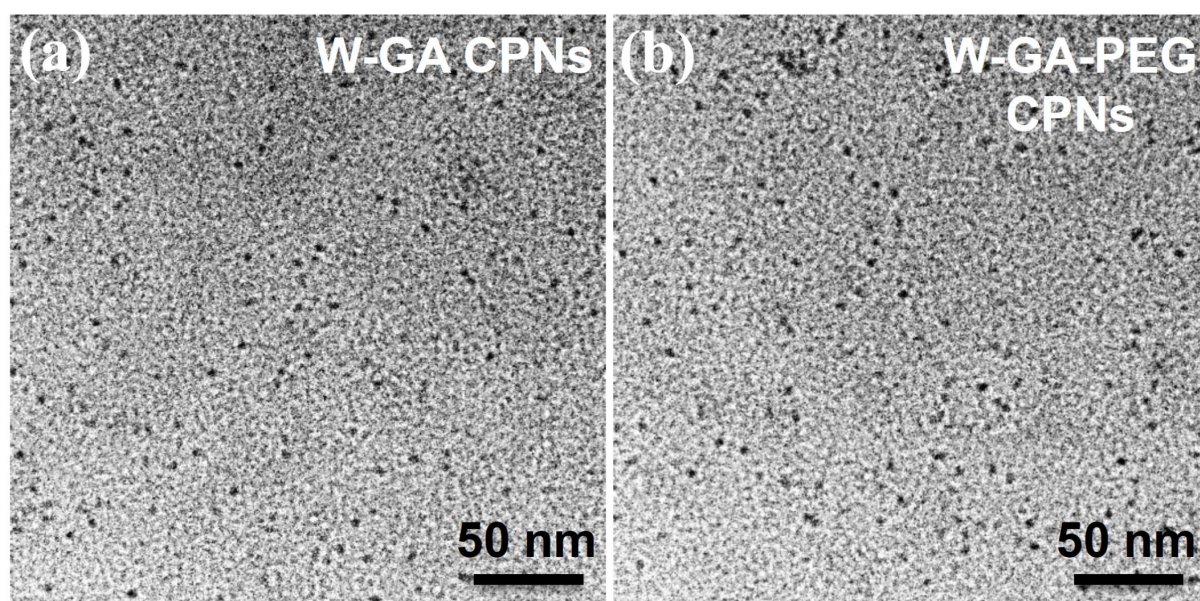
Supporting Figure S4. The EDX spectrum of the obtained W-GA CPNs.



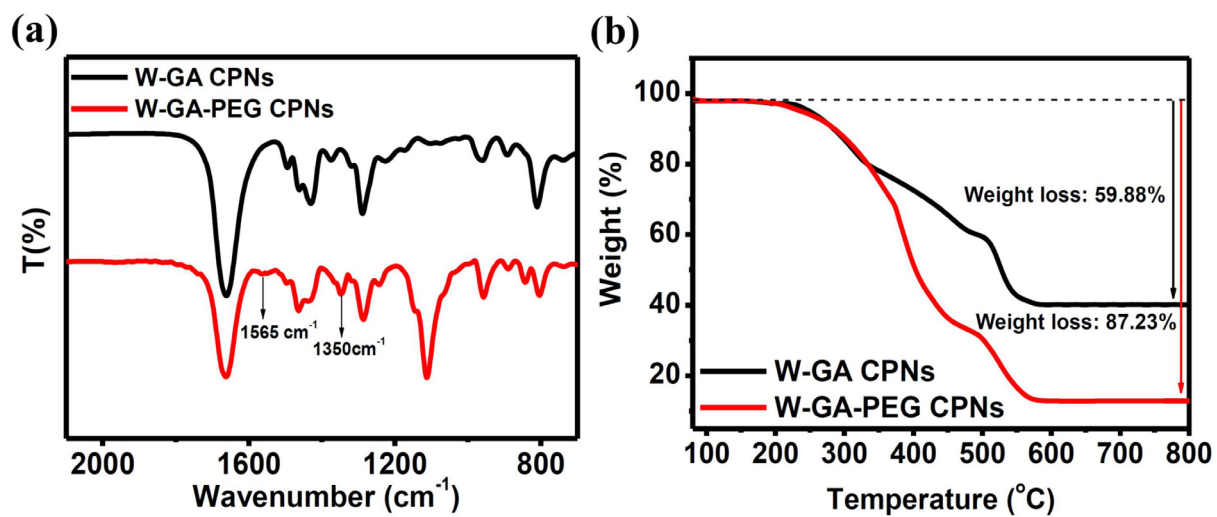
Supporting Figure S5. XPS spectra of (a) GA and (b) as-synthesized W-GA CPNs.



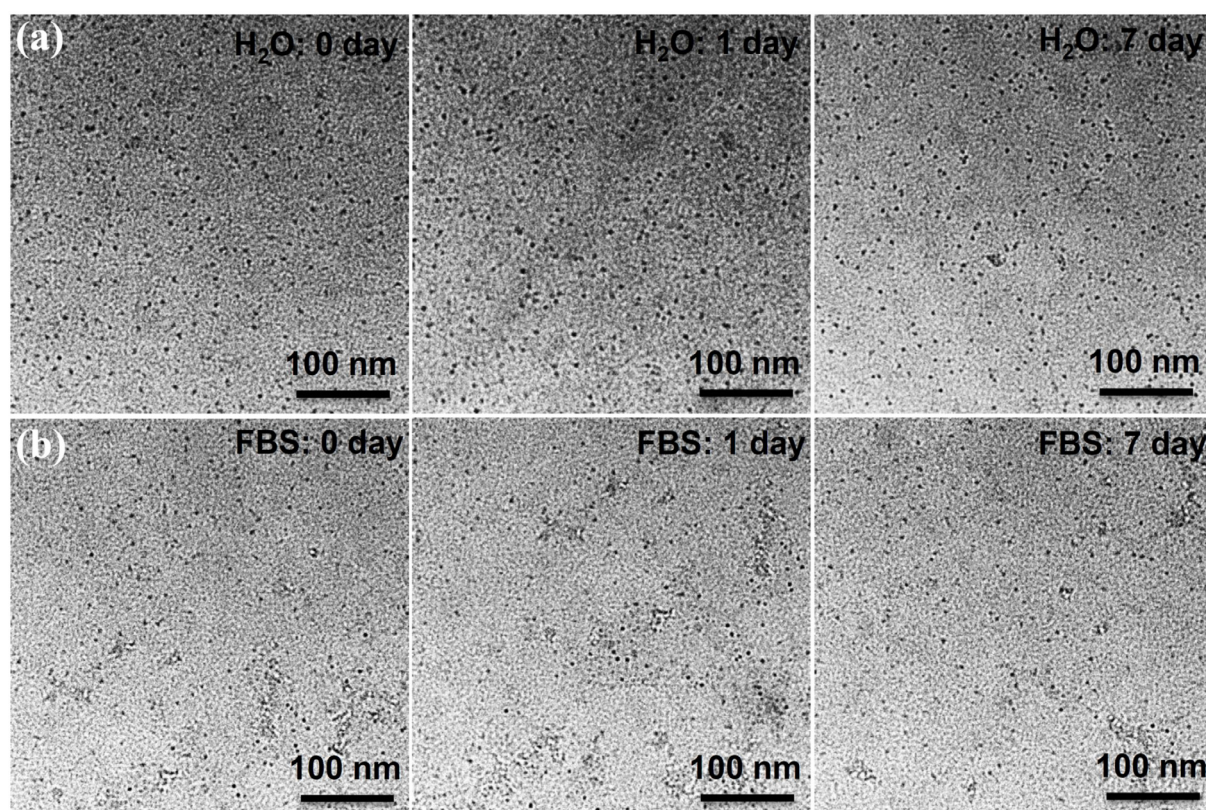
Supporting Figure S6. Fourier transform magnitude of k^3 -weighted W L_3 -edge extended X-ray absorption fine structure (EXAFS) spectra of the W-GA CPNs and WO_3 .



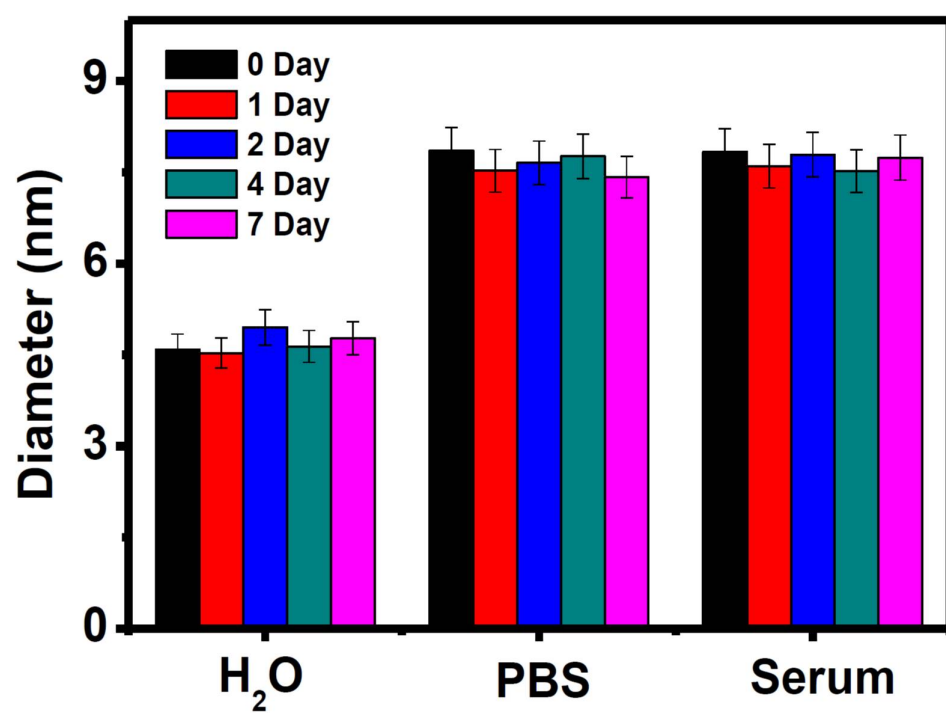
Supporting Figure S7. TEM images of W-GA CPNs (a) before and (b) after PEGylation.



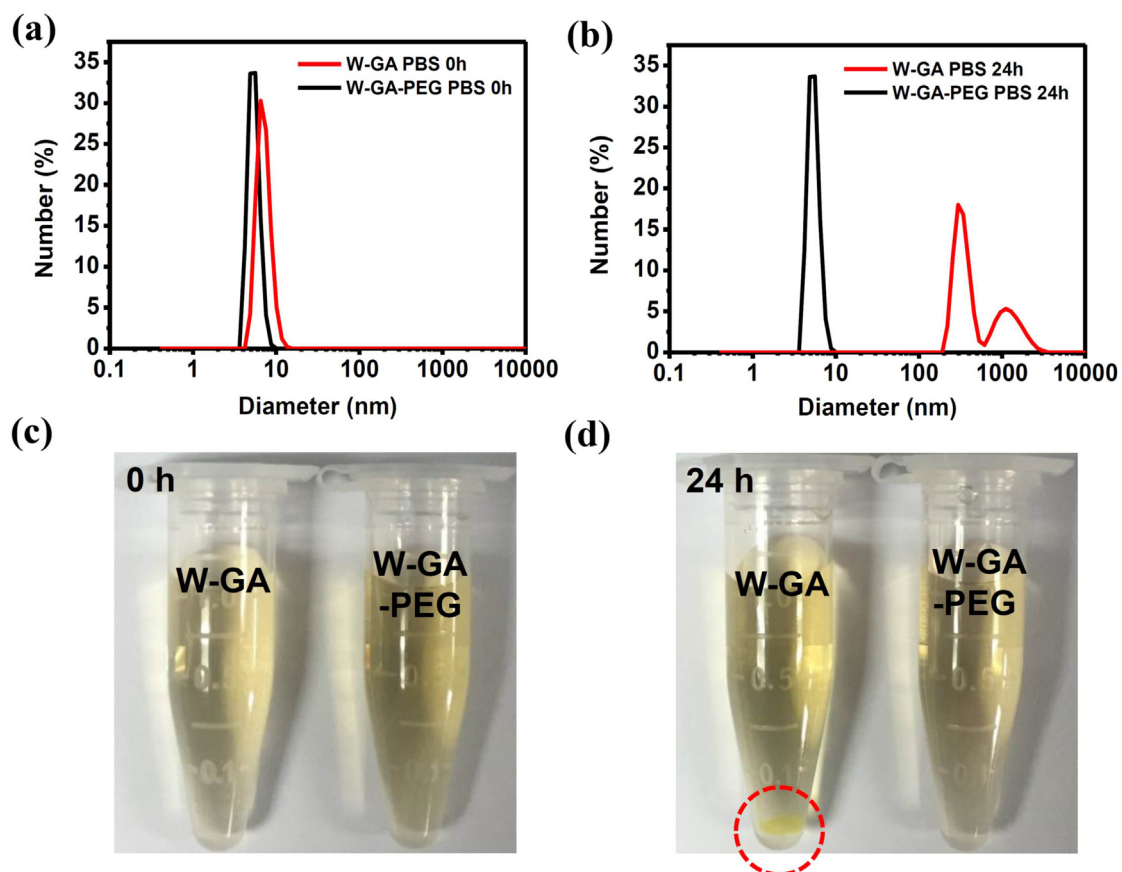
Supporting Figure S8. (a) FTIR spectra and (b) Thermogravimetric analysis (TGA) of as-synthesized W-GA CPNs before and after PEGylation.



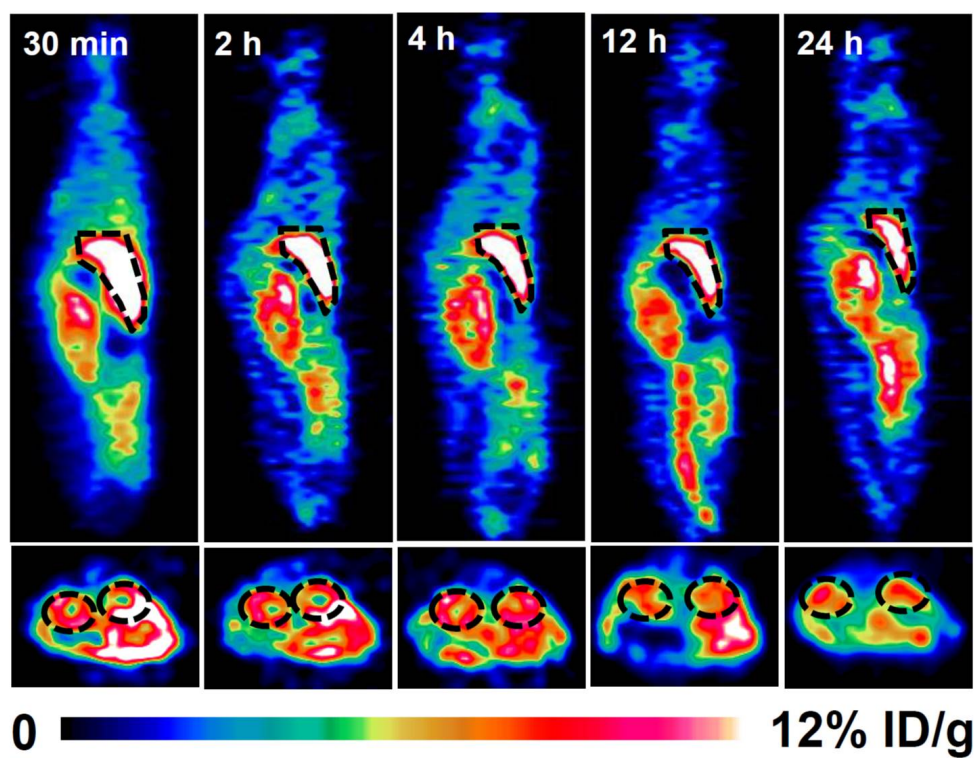
Supporting Figure S9. TEM images of PEGylated W-GA CPNs in water and FBS at various time points.



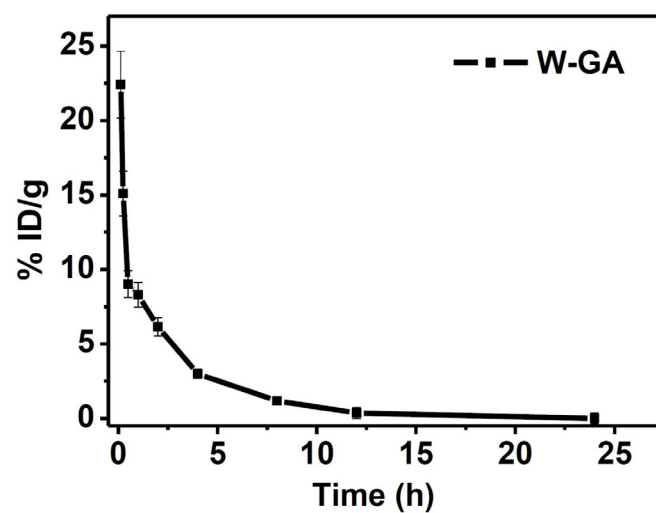
Supporting Figure S10. Stability test of PEGylated W-GA CPNs in water, PBS, and serum at various time points.



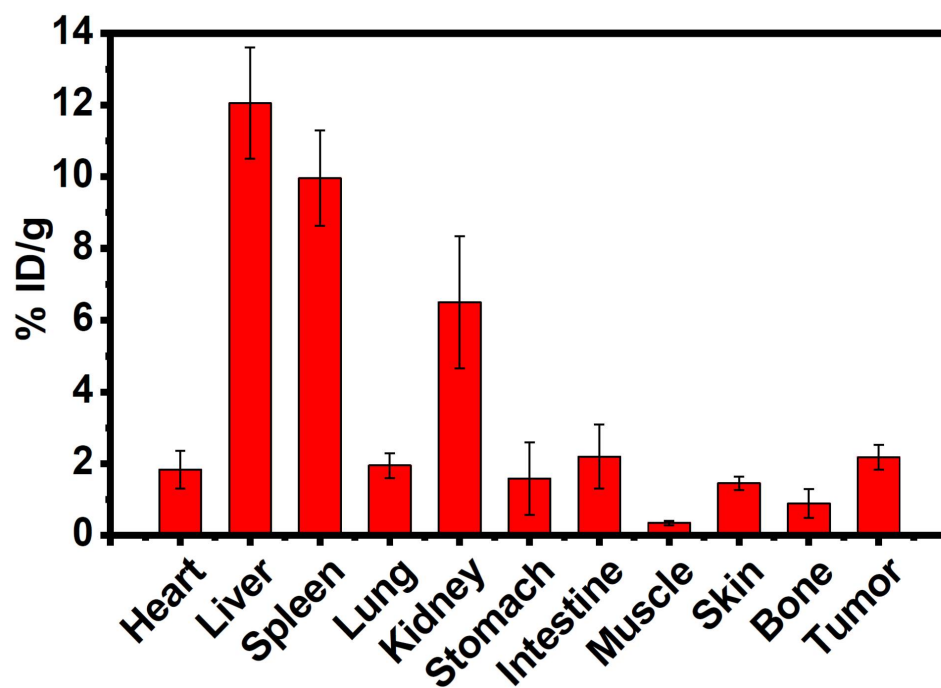
Supporting Figure S11. DLS-measured diameters of W-GA CPNs before and after PEGylation in PBS for 0 h (a) and 24 h (b). Photographs of W-GA CPNs and W-GA-PEG CPNs in PBS for 0 h (c) and 24 h (d).



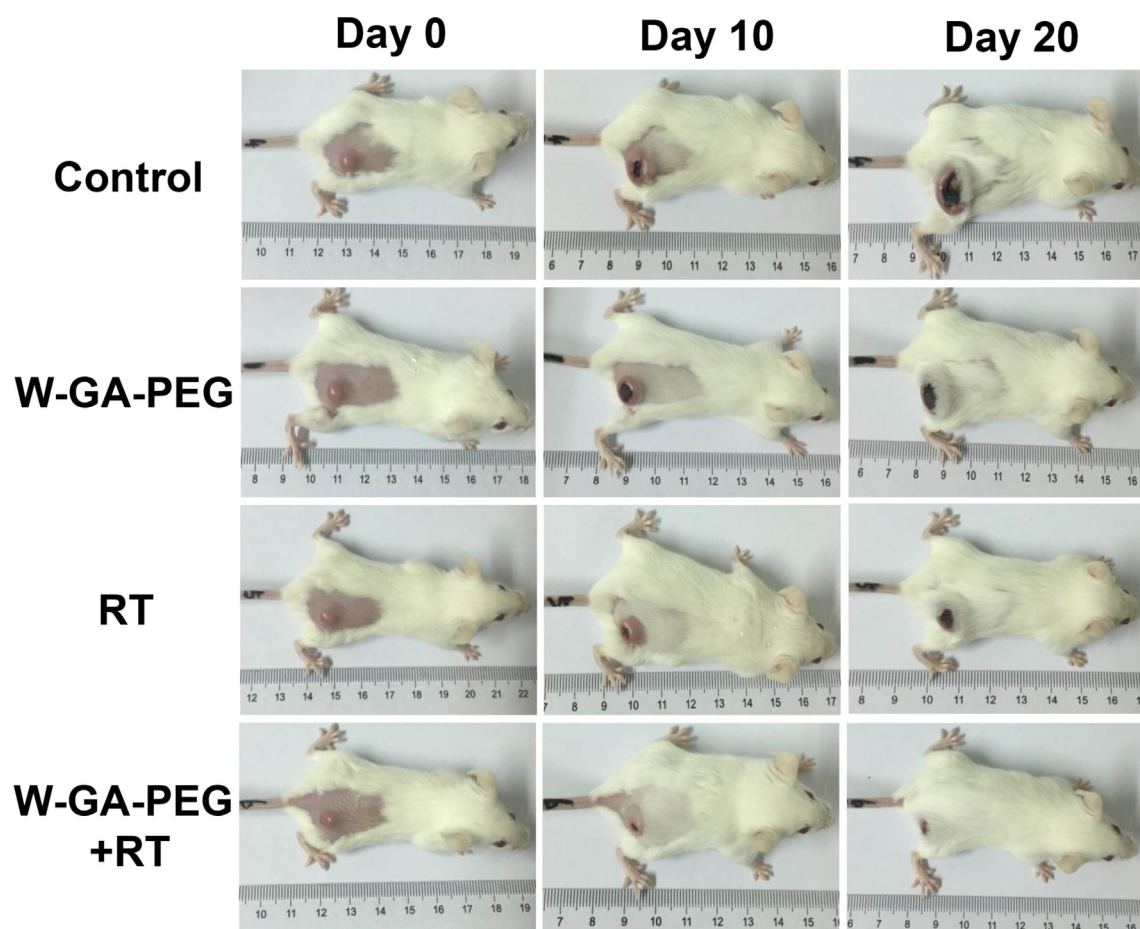
Supporting Figure S12. *In vivo* PET images of 4T1-tumor-bearing mice from different sections after *i.v.* injection of ^{64}Cu -W-GA-PEG CPNs taken at different time points. The liver and kidneys are indicated with black circles.



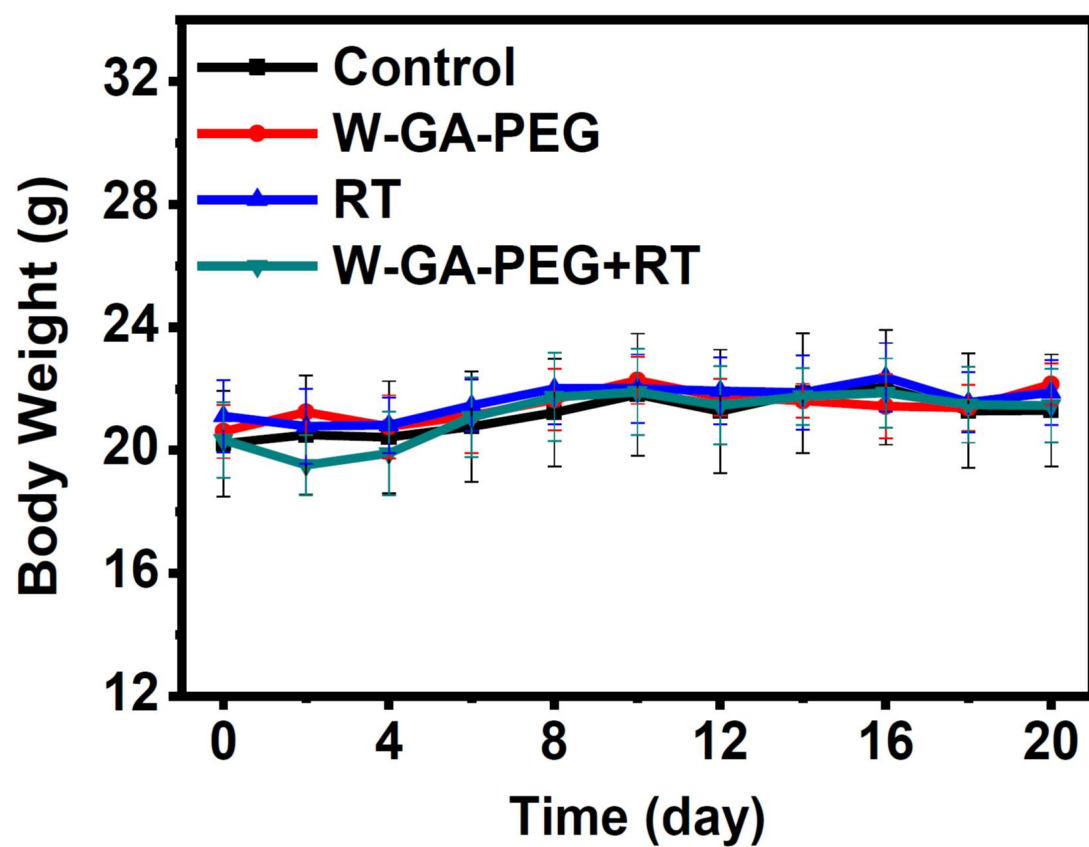
Supporting Figure S13. Blood circulation of W-GA-PEG CPNs in mice after *i.v.* injection measured by ICP-AES.



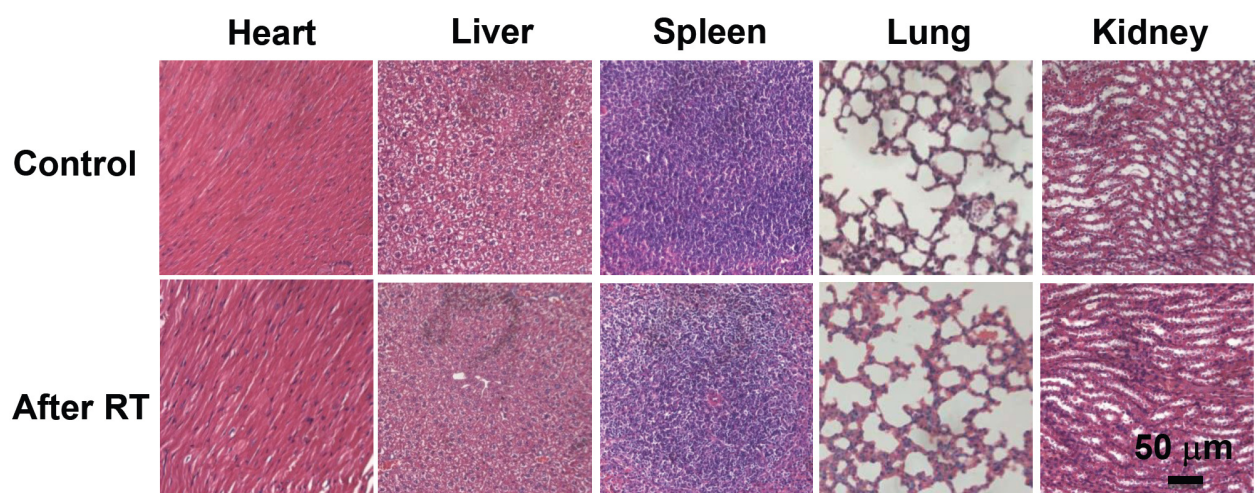
Supporting Figure S14. Biodistribution of ^{64}Cu -W-GA-PEG in various organs and tissues of 4T1 tumor-bearing mice at 24 h *p.i.* as determined by ^{64}Cu radioactivity measurement by a gamma counter.



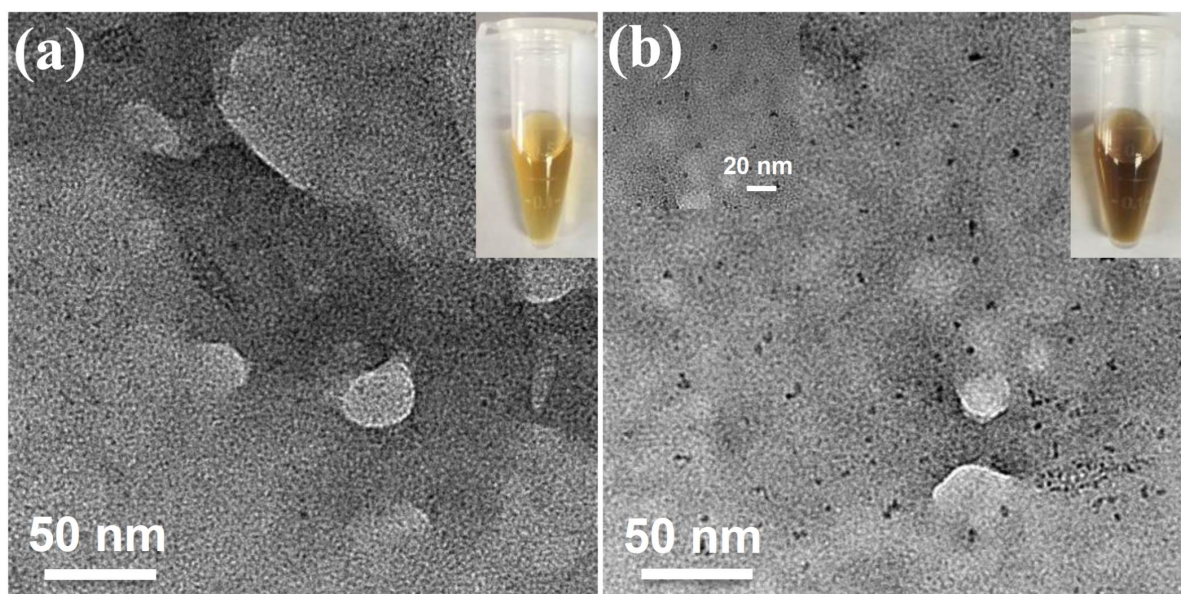
Supporting Figure S15. Representative photos of mice from different groups taken at 0, 10 days, and 20 days after various treatments.



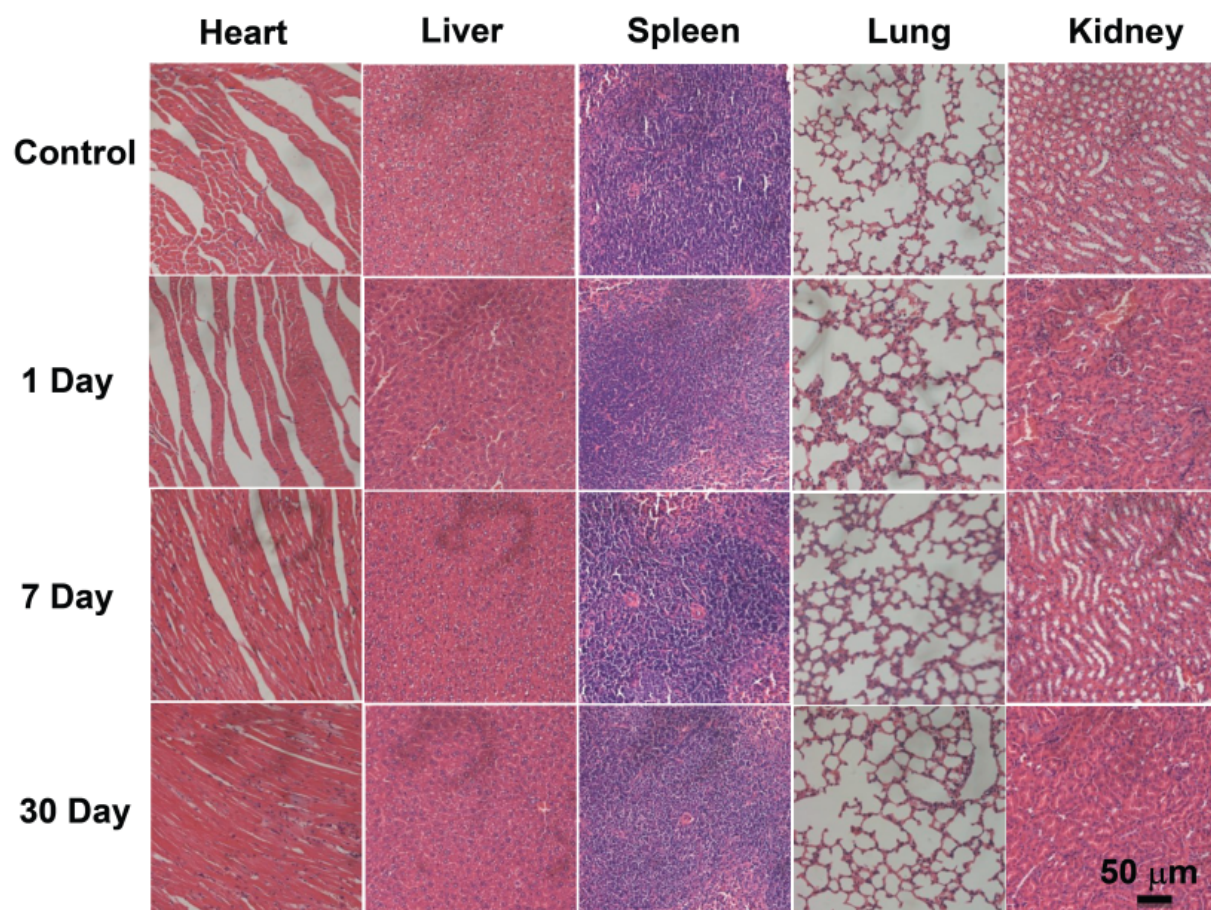
Supporting Figure S16. Body weight of mice after various treatments.



Supporting Figure S17. H&E stained slices of major organs of healthy untreated mice and mice 20 days post W-GA-PEG CPNs injection and radiotherapy.



Supporting Figure S18. TEM images of urine collected after 24 h from (a) untreated mice and (b) mice injected with W-GA-PEG CPNs. Insert: Photographs of urine collected from different groups.



Supporting Figure S19. H&E stained slices of major organs of healthy untreated mice and mice at the 1st day, 7th and 30th day post *i.v.* injection of W-GA-PEG CPNs.